Axisymmetric Eigenmodes Excited by Alpha Particle Energy Gradients in JET D-T Plasmas

Axisymmetric Eigenmodes Excited by Alpha Particle Energy Gradients in JET D-T Plasmas

H. J. C. Oliver,[1] D. King,[1] Ž. Štancar,[1] S. E. Sharapov,[1] D. Banerjee,[2] T. Barberis,[3] R. Coelho,[4] I. Coffey,[1] M. Dreval,[5] M. Fitzgerald,[1] L. Frassinetti,[6] C. Giroud,[1] N. Hawkes,[1] D. Keeling,[1] C. C. Kim,[7] E. Lerche,[8] F. Porcelli,[2] and G. Szepesi[1]

JET Contributors[*]

EUROfusion Tokamak Exploitation Team[†]

[1]*United Kingdom Atomic Energy Authority, Culham Campus, Abingdon, Oxfordshire, OX14 3DB, United Kingdom*
[2]*Department of Applied Science and Technology, Polytechnic University of Turin, Torino 10129, Italy*
[3]*Princeton Plasma Physics Laboratory, Princeton University, Princeton, New Jersey 08543, USA*
[4]*Instituto de Plasmas e Fusão Nuclear, Instituto Superior Técnico, Universidade de Lisboa, Lisboa, Portugal*
[5]*National Science Centre, Kharkiv Institute of Physics and Technology, 61108 Kharkiv, Ukraine*
[6]*Division of Electromagnetic Engineering and Fusion Science, KTH Royal Institute of Technology, Stockholm SE-100 44, Sweden*
[7]*SLS2 Consulting, San Diego, California 92107, USA*
[8]*Laboratory for Plasma Physics, ERM/KMS, B-1000 Brussels, Belgium*

(Received 23 July 2025; accepted 17 December 2025; published 4 February 2026)

Axisymmetric Alfvén eigenmodes have been observed at the plasma edge in deuterium-tritium (D-T) tokamak plasmas externally heated only by neutral beam injection in JET. The modes were detected only in D-T plasmas, not in pure D plasmas, indicating excitation by fusion-born α particles. The presence of the axisymmetric mode suggests that the modes were driven by positive energy gradients in the α particle distribution rather than radial gradients. The modes are driven by counter-current passing α particles with large orbit widths, allowing core-born α particles to interact with modes at the plasma edge. This reveals an excitation mechanism arising from positive energy gradients produced by the minimum energy required to confine particles at the edge, relevant to all burning plasmas.

DOI: 10.1103/j3cm-5mtm

Interactions between energetic particles and Alfvén waves play a critical role in determining the behavior of magnetized plasmas across laboratory and astrophysical environments. In magnetically confined fusion plasmas, Alfvén eigenmodes can degrade performance or damage plasma-facing components [1] by redistributing fast particles, but they may also suppress turbulence and enhance confinement [2]. These modes are destabilized by resonant energy transfer from energetic particles due to gradients in their distribution, which is described by the constants of motion: energy E, canonical toroidal angular momentum P_ϕ, and the magnetic moment μ. Alfvén eigenmodes interacting with different gradients transport energetic particles in distinct ways and require tailored mitigation strategies [3].

Fusion research is entering the era of "burning plasmas," as reactors worldwide prepare to operate with plasmas directly heated by fusion-born α particles. However, α particles may also destabilize Alfvén eigenmodes, as observed in the Tokamak Fusion Test Reactor [4,5] and Joint European Torus [6], where P_ϕ (radial) gradients excited modes in afterglow experiments [7]. Despite dedicated experiments to produce positive α particle energy gradients at suprathermal energies using beam modulation, the observed modes were not destabilized by these bump-on-tail distributions [8,9].

Noether's theorem reveals that P_ϕ is conserved in a toroidally symmetric field. Therefore, axisymmetric modes (toroidal mode number $n = 0$) cannot perturb the P_ϕ of a particle and must be driven by either energy or μ (anisotropy) gradients. Axisymmetric global Alfvén

[*]See author list of C. F. Maggi *et al.*, Overview of T and D–T results in JET with ITER-like wall, Nucl. Fusion 64, 112012 (2024).
[†]See author list of E. Joffrin *et al.*, Overview of the EUROfusion tokamak exploitation programme in support of ITER and DEMO, Nucl. Fusion 64, 112019 (2024).

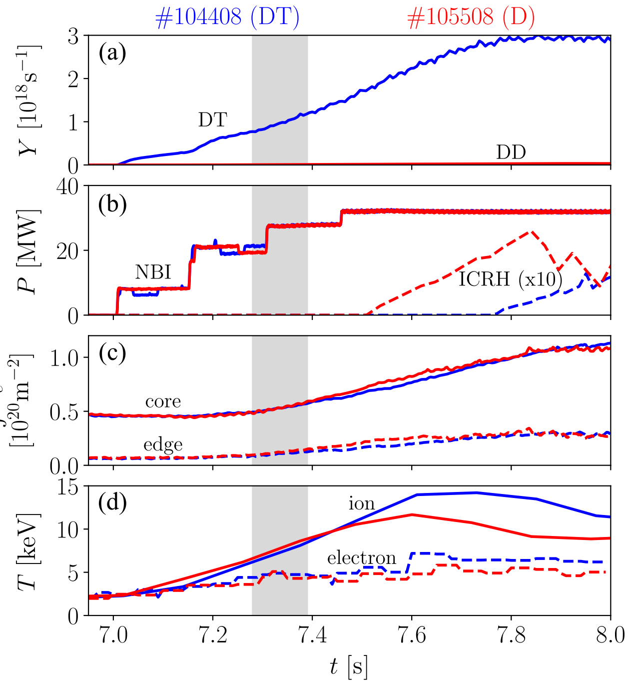

FIG. 1. Time evolution of parameters in D-T plasma 104408 (blue) and pure D plasma 105508 (red): (a) neutron yield, (b) auxiliary heating power, (c) line integrated electron density, and (d) ion and electron temperature at $R = 3.3$ m. The gray box shows the time of mode excitation.

eigenmodes [10–13] have been observed in pure D and $D-He^3$ JET plasmas heated by MeV deuterons accelerated with ion cyclotron resonance heating (ICRH) [14–16], although the highly anisotropic and energetic ICRH ions made it difficult to unambiguously determine the source of drive.

In this Letter, we report the observation of axisymmetric modes driven by energy gradients in the α particle distribution in D-T plasmas heated exclusively by neutral beam injection without ICRH. The wave electric field peaks at the edge of the plasma, yet the waves were destabilized by α particles born in the core with drift orbit excursions large enough to reach the edge. This result establishes drive from α particle energy gradients as an effective excitation mechanism in reactor-relevant plasmas.

The modes were excited in several hybrid scenario D-T plasmas [17] heated with high-power beam injection to investigate tungsten impurity screening [18]. Although not optimized for the study of Alfvén eigenmodes, these conditions produced high fusion yields, providing ideal conditions for studying α effects. The axisymmetric modes were observed in several pulses with on-axis magnetic fields $B_0 = 3.85$ T, but not in similar plasmas with $B_0 = 3.45$ T. JET plasma #104408—characterized by the major radius at the magnetic axis $R_0 = 2.9$ m, minor radius 0.9 m, and relatively low plasma current $I_p = 2.1$ MA—was selected for detailed analysis due to its comprehensive diagnostic coverage. The initial fuel ion mix was approximately 20/80 D/T, but the mix began equalizing from 7.5 s. Key time traces are shown in Fig. 1. The plasma was heated with deuterium beam injection at a maximum energy 113 keV, with the power increasing in steps up to 31 MW at 7.46 s. The plasma was heated with ICRH from 7.76 s, after the modes were observed. The rapidly increasing D beam ion density and T-rich plasma led to a sharp rise in the fusion rate up to 3×10^{18} s^{-1}, corresponding to a fusion power of 8.4 MW.

Coherent electromagnetic modes were detected in the toroidal Alfvén eigenmode frequency range on magnetic coil spectrograms prior to the onset of ICRH, as demonstrated in Fig. 2. The mode amplitudes were sufficiently strong to appear on multiple toroidally separated coils, enabling the determination of their toroidal mode numbers, which are shown in Fig. 3. In previous JET D-T campaigns, alpha-driven modes were either too faint to calculate the toroidal mode numbers [6] or were not observed by magnetic coils [8,9]. The $n = 0$ mode was destabilized from 7.28 to 7.37 s, while the $n = +1$ (co-current) mode was destabilized from 7.32 to 7.39 s. Additionally, the modes were measured on several sightlines of the soft x-ray camera.

Edge localized modes (ELMs) strongly modulated the frequency and amplitude of the observed modes, as shown in Fig. 2. However, the ELMs did not significantly affect the core density, core or edge temperature, or ion concentrations. Only the edge density was perturbed by the ELMs. The modulation of the Alfvénic modes by these weak perturbations indicates that there was significant mode structure at the plasma edge.

Both beam ions and α particles can resonate with the observed modes. To identify the source of drive, the D-T plasma was repeated using a pure D plasma only. All other plasma parameters, including the heating power, plasma current, magnetic field, and gas injection were controlled in the D reference plasma 105508 to replicate the conditions of D-T plasma 104408, as demonstrated in Fig. 1. The density and q profiles are very similar in the two plasmas, and the resulting ELM and low frequency magnetohydrodynamic (MHD) activity match, as shown in Fig. 2. However, without a significant population of fusion-born α particles, the modes present in the D-T plasma were not observed in the pure D reference plasma. This indicates that the modes observed in the D-T plasma were driven unstable by α particles.

To confirm the source of drive for the observed mode, the wave-particle interaction was numerically modeled at time $t = 7.35$ s in D-T plasma 104408 using inputs [19] from the validated integrated modeling workflow described in Ref. [20]. The linear, ideal MHD code MISHKA-1 [21] was used to compute the eigenfrequencies and spatial structures of the observed modes. The $n = 1$ mode is identified as a toroidal Alfvén eigenmode. The $n = 0$ mode, which is the focus of this Letter, is a global Alfvén eigenmode with an eigenfrequency 191 kHz, which is higher than the

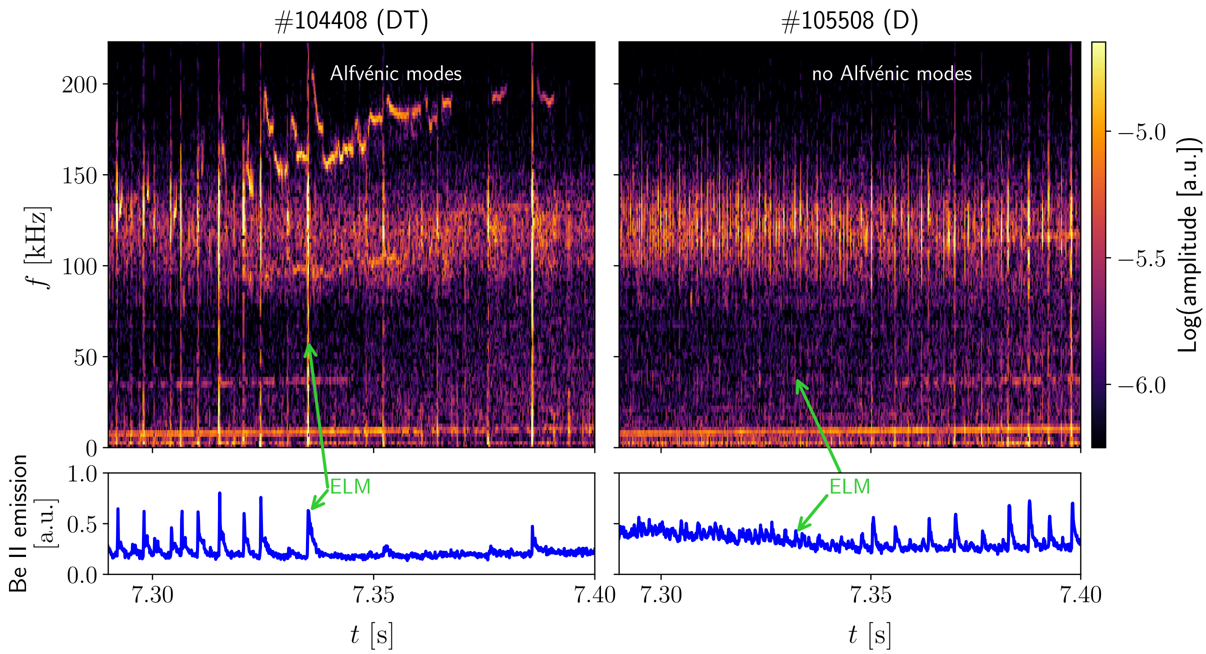

FIG. 2. Top: spectrogram of D-T plasma 104408 and pure D plasma 105508 showing the amplitude of the perturbed magnetic field. Bottom: Be II 527 nm emission at the divertor. ELMs appear as bright, vertical lines in the magnetic spectrogram and as spikes in Be II emission.

experimental value of 171 kHz due to uncertainties in the impurity composition and the edge q profile. The global Alfvén eigenmode lies below the lowest minimum of the Alfvén continuum and has an antiballooning (odd) parity, with coupled dominant poloidal harmonics $m = \pm 1$ of opposite sign [14]. Consequently, the eigenmode is located on the high-field-side of the tokamak (at low major radius R). While the electrostatic potential is global, the electric field is highly peaked at the plasma edge, where steep gradients in density and the safety factor profile combine to form a potential well that localizes the Alfvén wave. This is consistent with the inference from experimental observations that the mode electric field is located at the plasma edge.

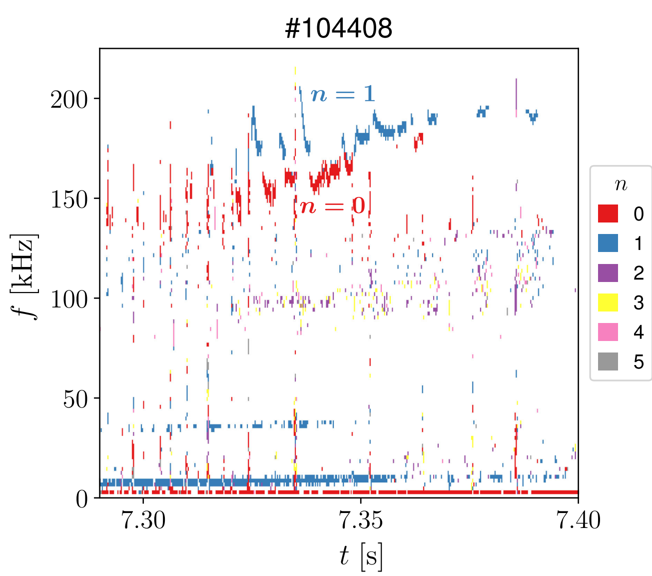

FIG. 3. Phase spectrogram of magnetic data showing toroidal mode numbers n of coherent signals in pulse 104408.

Vertical displacement oscillatory modes [22,23] could exist in a similar frequency range. The extended MHD initial value code NIMROD [24] can model vertical displacement oscillatory modes because it includes an open field line region beyond the plasma separatrix, which is absent in MISHKA for $n = 0$. When the wall is positioned at the separatrix, both MHD codes find the same eigenmode structure. As the wall moves away from the plasma, the frequency of the mode decreases. The frequency of the computed mode decreases with increasing edge density gradient, consistent with the experimental observation of downward frequency sweeping as the density at the edge collapses and recovers over an ELM cycle.

This mode has been identified as a global Alfvén eigenmode in Refs. [13–15,25] and as a vertical displacement oscillatory mode in Ref. [16]. However, both MHD codes compute the same eigenmode structure, and the difference in interpretation does not affect the stability analysis. The power transfer between the axisymmetric eigenmode and fast particles was calculated using the HALO code [26]. The distributions functions of the energetic particles were calculated by following their full orbits from birth until thermalization using the LOCUST code [27,28], which solves the Lorentz force equation and applies a collision operator for a sufficient numbers of particles to

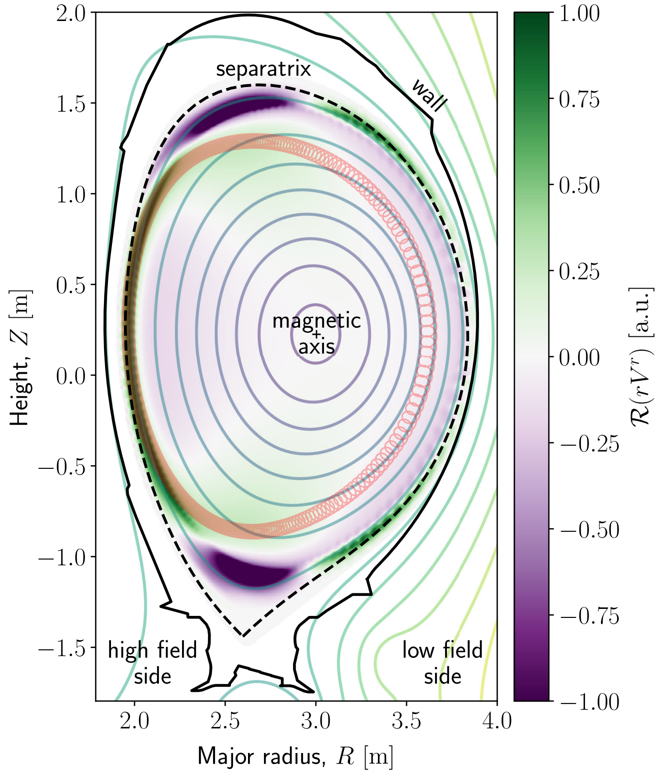

FIG. 4. Typical orbit of a highly resonant counterpassing α particle in red (followed by HALO and LOCUST) superimposed on the real part of the perturbed radial velocity rV^r of the mode computed with MISHKA.

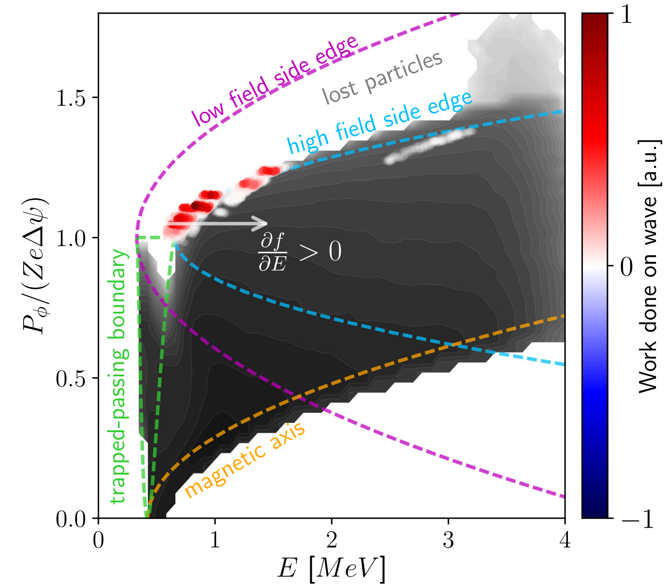

FIG. 5. Contours of the LOCUST counter-current α particle distribution for $100 \leq \mu[\mathrm{keV/T}] \leq 125$ in gray scale. Highly resonant α particles from HALO are overlaid, with red denoting drive and blue representing damping. Dashed lines show approximate orbit topological boundaries [29]. An animated version of this figure is available in the supplemental material [30].

compute smooth distribution functions suitable for kinetic stability calculations [9].

Fusion-born α particles in JET have large orbits that deviate significantly from flux surfaces, particularly due to the relatively low plasma current and high edge safety factor q. This allows α particles born at midradius to reach the plasma edge, where they interact with the mode, as shown by Fig. 4. Alpha particles that have slowed to lower energies have narrower orbits and are unable to reach the edge. This depletes the low energy portion of the α particle distribution function at the edge, creating a local, stable population inversion in the energy distribution.

The α particle population drives the $n = 0$ mode with a growth rate $\gamma_\alpha/\omega = +3.1 \times 10^{-3}$. Almost all wave-particle interaction occurs at the plasma edge. The power transfer is dominated by counter-current passing particles, which drift toward the high-field-side edge of the tokamak where the wave electric field peaks, as demonstrated by Fig. 4. Parallel motion slows significantly on the high-field side of the tokamak and the α particle spends a majority of the poloidal transit period in the wave electric field. This extended interaction enables the efficient transfer of energy from α particles to the wave.

Figure 5 shows a $E - P_\phi$ slice of the counter-current α particle distribution at constant μ. Particles must exceed a minimum energy to remain confined by the magnetic field. Sufficiently energetic particles remain inside the high-field-side separatrix, while lower energy particles drift outside and impact the reactor wall. As a result, a sharp transition in the energy distribution exists at this confinement boundary. This threshold produces a local positive energy gradient at suprathermal energies—a bump-on-tail distribution—for particles with finite magnetic moment $\mu > 0$ and $P_\phi \gtrsim Ze\Delta\psi$, where $\Delta\psi$ is the difference in magnetic flux ψ between the edge and core, $P_\phi \equiv mRv_\phi + Ze\psi$ and m, R, v_ϕ, and Ze are the particle mass, major radius, toroidal velocity, and charge. This energy gradient provides the free energy driving the waves in our experiment through inverse Landau damping. The energy confinement threshold increases with μ and so the local energy population inversion can drive the wave through many resonances at $0.1 \lesssim E[\mathrm{MeV}] \lesssim 4.0$ when all values of μ are considered. The high-field-side edge and the associated positive energy gradient exist in all tokamak plasmas, and does not require a time dependent source.

The beam ions damp the eigenmode at a rate $\gamma_b/\omega = -2.2 \times 10^{-3}$. The majority of the beam ion Landau damping occurs at the half-energy injection, ~55 keV, where strong negative energy gradients occur due to the beam source. As for the α particles, the vast majority of the power transfer occurs at the plasma periphery. However, the lower energy and narrower orbit widths of the beam ions limit their ability to reach and interact with the wave electric field located at the edge. In addition, the majority of beam ions are copassing and drift toward the low-field side of the tokamak, away from the peak of the wave field.

The ion Landau damping from both thermal D and T ions was evaluated by loading Maxwellian distributions into HALO in place of the fast particle distribution function. The resulting damping rates were $\gamma_D/\omega = -2.0 \times 10^{-4}$ and $\gamma_T/\omega = -3.5 \times 10^{-4}$, respectively. Additional damping mechanisms are modeled using complex resistivity in CASTOR [31–33], a resistive MHD code that computes the eigenmodes present in a tokamak plasma. Radiative damping [34] $\gamma_{rad}/\omega = -3.9 \times 10^{-5}$ and collisional damping [35] $\gamma_{coll}/\omega = -3.2 \times 10^{-5}$ are an order of magnitude smaller than the ion Landau damping rate and only slowly dissipate the mode energy because the thermal electrons are relatively cool at the plasma edge. Continuum damping [36] $\gamma_{cont}/\omega = -1.2 \times 10^{-6}$ is weak due to the strong magnetic shear at the plasma edge, which separates the global Alfvén eigenmode from the Alfvén continuum. Furthermore, the mode is near only a single Alfvén continuum branch, with the next nearest branch near twice the eigenfrequency due to the high plasma ellipticity at the edge [14].

The high magnetic field in this plasma increased the Alfvén velocity v_A, and the mode location on the high-field-side edge further enhanced the local v_A. As a result, Landau damping by the relatively slow thermal and beam ions was limited to inefficient sideband resonances. Conversely, the super-Alfvénic α particles were sufficiently energetic to resonate through both principal and sideband resonances. The dependence of the resonance conditions on the magnetic field may explain why no waves were detected in similar plasmas at lower magnetic field $B_0 = 3.45$ T.

Combining the drive from α particles with all damping mechanisms, the net growth rate of the $n = 0$ mode observed during the third JET D-T campaign is $\gamma/\omega = +2.1 \times 10^{-4}$. This is close to marginal stability, which is consistent with the transient excitation of the mode. However, the positive energy gradients are present in a steady state distribution of α particles. The transient mode excitation is caused by an increase in damping as the plasma temperature increases. The local positive energy gradients are not transient like many bump-on-tail distributions, for example, those produced by beam modulation [3,8] in a tokamak, by magnetic reconnection in the magnetotail [37], in type III solar radio emission [38], or in optical systems [39].

The mode was destabilized by steep positive energy gradients that naturally occur due to the minimum energy required to confine a particle at the edge. The energy gradient at the high-field-side separatrix—along with similar inherent positive energy gradients at the magnetic axis and low-energy threshold of the trapped-passing boundary—will be present in future burning plasmas and may drive axisymmetric or nonaxisymmetric modes.

The large orbits of α particles in JET, resulting from low plasma current and high edge q, enabled power transfer with the mode at the plasma periphery. Many future reactors plan to operate at high q to avoid performance-limiting MHD instabilities, which will produce similarly large α particle orbit excursions and enhance mode drive. Additionally, the broad thermonuclear fusion reactivity profiles planned for many reactors will produce appreciable α particle populations beyond midradius, increasing the power transfer to modes at the edge.

While axisymmetric modes do not induce radial transport, they can cause energy diffusion sufficient to degrade fast particle confinement near the trapped-passing boundary or plasma edge. The drive mechanism identified here can also excite nonaxisymmetric modes to amplitudes sufficient for radial transport.

Axisymmetric modes may also play a positive role in tokamak plasmas. Energy extracted from α particles born at midradius is channeled [40] by modes to thermal fuel ions at the plasma edge, offering a potential mechanism to enhance plasma heating in future burning plasmas. Axisymmetric Alfvén eigenmodes have also been shown to interact strongly with microturbulence [41], suggesting they can play a role in the regulation of turbulence, potentially improving confinement in tokamak plasmas.

Acknowledgments—The authors thank F. Camilo de Souza, K. McClements, and anonymous referees for improving this manuscript. This work has been carried out within the framework of the EUROfusion Consortium, funded by the European Union via the Euratom Research and Training Programme (Grant Agreement No. 101052200—EUROfusion) and from the EPSRC (Grant No. EP/W006839/1). To obtain further information on the data and models underlying this paper please contact PublicationsManager@ ukaea.uk.

Views and opinions expressed are, however, those of the author(s) only and do not necessarily reflect those of the European Union or the European Commission. Neither the European Union nor the European Commission can be held responsible for them.

Data availability—The data that support the findings of this article are openly available [19].

[1] H. H. Duong, W. W. Heidbrink, E. J. Strait, T. W. Petrie, R. Lee, R. A. Moyer, and J. G. Watkins, Loss of energetic beam ions during TAE instabilities, Nucl. Fusion **33**, 749 (1993).

[2] A. Di Siena, T. Görler, E. Poli, A. Bañón Navarro, A. Biancalani, and F. Jenko, Electromagnetic turbulence suppression by energetic particle driven modes, Nucl. Fusion **59**, 124001 (2019).

[3] M. A. Van Zeeland, L. Bardoczi, J. Gonzalez-Martin, W. W. Heidbrink, M. Podesta, M. Austin, C. S. Collins, X. D. Du,

V. N. Duarte, M. Garcia-Munoz, S. Munaretto, K. E. Thome, Y. Todo, and X. Wang, Beam modulation and bump-on-tail effects on Alfvén eigenmode stability in DIII-D, Nucl. Fusion **61**, 066028 (2021).

[4] R. Nazikian *et al.*, Alpha-particle-driven toroidal Alfvén eigenmodes in the Tokamak Fusion Test Reactor, Phys. Rev. Lett. **78**, 2976 (1997).

[5] R. Nazikian, G. J. Kramer, C. Z. Cheng, N. N. Gorelenkov, H. L. Berk, and S. E. Sharapov, New interpretation of alpha-particle-driven instabilities in deuterium-tritium experiments on the Tokamak Fusion Test Reactor, Phys. Rev. Lett. **91**, 125003 (2003).

[6] M. Fitzgerald *et al.*, Stability analysis of alpha driven toroidal Alfvén eigenmodes observed in JET deuterium-tritium internal transport barrier plasmas, Nucl. Fusion **63**, 112006 (2023).

[7] G. Y. Fu, C. Z. Cheng, R. Budny, Z. Chang, D. S. Darrow, E. Fredrickson, E. Mazzucato, R. Nazikian, K. L. Wong, and S. Zweben, Analysis of alpha particle-driven toroidal Alfvén eigenmodes in Tokamak Fusion Test Reactor deuterium–tritium experiments, Phys. Plasmas **3**, 4036 (1996).

[8] S. E. Sharapov *et al.*, Experiments on excitation of Alfvén eigenmodes by alpha-particles with bump-on-tail distribution in JET DTE2 plasmas, Nucl. Fusion **63**, 112007 (2023).

[9] H. J. C. Oliver, S. E. Sharapov, Ž. Štancar, M. Fitzgerald, E. Tholerus, B. N. Breizman, M. Dreval, J. Ferreira, A. Figueiredo, J. Garcia, N. Hawkes, D. L. Keeling, P. G. Puglia, P. Rodrigues, R. A. Tinguely, and JET Contributors, Toroidal Alfvén eigenmodes observed in low power JET deuterium–tritium plasmas, Nucl. Fusion **63**, 112008 (2023).

[10] D. W. Ross, G. L. Chen, and S. M. Mahajan, Kinetic description of Alfvén wave heating, Phys. Fluids **25**, 652 (1982).

[11] K. Appert, R. Gruber, .F Troyuon, and J. Vaclavik, Excitation of global eigenmodes of the Alfvén wave in tokamaks, Plasma Phys. **24**, 1147 (1982).

[12] A. de Chambrier, A. D. Cheetham, A. Heym, F. Hofmann, B. Joye, R. Keller, A. Lietti, J. B. Lister, and A. Pochelon, Alfvén wave coupling experiments of the TCA tokamak, Plasma Phys. **24**, 893 (1982).

[13] L. Villard and J. Vaclavik, Alfvén frequency modes and global Alfvén eigenmodes, Nucl. Fusion **37**, 351 (1997).

[14] H. J. C. Oliver, S. E. Sharapov, B. N. Breizman, and L.-J. Zheng, Axisymmetric global Alfvén eigenmodes within the ellipticity-induced frequency gap in the joint european torus, Phys. Plasmas **24**, 122505 (2017).

[15] V. G. Kiptily *et al.*, Excitation of Alfvén eigenmodes by fusion-born alpha-particles in D-^{3}He plasmas on JET, Plasma Phys. Controlled Fusion **64**, 064001 (2022).

[16] T. Barberis, C. C. Kim, F. Porcelli, D. Banerjee, N. Hawkes, Ye O. Kazakov, Y. Q. Liu, H. J. C. Oliver, S. E. Sharapov, A. Yolbarsop, NIMROD Team, and JET Contributors, Simulations of vertical displacement oscillatory modes and global Alfvén eigenmodes in JET geometry, Nucl. Fusion **64**, 126064 (2024).

[17] J. Hobirk *et al.*, The JET hybrid scenario in deuterium, tritium and deuterium-tritium, Nucl. Fusion **63**, 112001 (2023).

[18] C. Angioni, Impurity transport in tokamak plasmas, theory, modelling and comparison with experiments, Plasma Phys. Controlled Fusion **63**, 073001 (2021).

[19] H. J. C. Oliver, Zenodo repository, 2026, 10.5281/zenodo.18154650.

[20] Ž. Štancar *et al.*, Overview of interpretive modelling of fusion performance in JET DTE2 discharges with TRANSP, Nucl. Fusion **63**, 126058 (2023).

[21] A. B. Mikhailovskii, G. T. A. Huysmans, W. O. K. Kerner, and S. E. Sharapov, Optimization of computational MHD normal-mode analysis for tokamaks, Plasma Phys. Rep. **23**, 844 (1997).

[22] T. Barberis, A. Yolbarsop, and F. Porcelli, Vertical displacement oscillatory modes in tokamak plasmas, J. Plasma Phys. **88**, 905880511 (2022).

[23] T. Barberis, F. Porcelli, and A. Yolbarsop, Fast-ion-driven vertical modes in magnetically confined toroidal plasmas, Nucl. Fusion **62**, 064002 (2022).

[24] C. R. Sovinec, A. H. Glasser, T. A. Gianakon, D. C. Barnes, R. A. Nebel, S. E. Kruger, D. D. Schnack, S. J. Plimpton, A. Tarditi, and M. S. Chu, Nonlinear magnetohydrodynamics simulation using high-order finite elements, J. Comput. Phys. **195**, 355 (2004).

[25] K. G. McClements, L. C. Appel, M. J. Hole, and A. Thyagaraja, Excitation of axisymmetric Alfvénic modes in ohmic tokamak discharges, Nucl. Fusion **42**, 1155 (2002).

[26] M. Fitzgerald, J. Buchanan, R. J. Akers, B. N. Breizman, and S. E. Sharapov, HALO: A full-orbit model of nonlinear interaction of fast particles with eigenmodes, Comput. Phys. Commun. **252**, 106773 (2020).

[27] R. J. Akers, E. Verwichte, T. J. Martin, S. D. Pinches, and R. Lake, GPGPU Monte Carlo calculation of gyro-phase resolved fast ion and n-state resolved neutral deuterium distributions, *Proceedings of the 39th EPS Conference and 16th International Congress on Plasma Physics* (Stockholm, Sweden, 2012), pp. P5.088:3217–3226.

[28] S. H. Ward, R. Akers, A. S. Jacobsen, P. Ollus, S. D. Pinches, E. Tholerus, R. G. L. Vann, and M. A. Van Zeeland, Verification and validation of the high-performance Lorentz-orbit code for use in stellarators and tokamaks (LOCUST), Nucl. Fusion **61**, 086029 (2021).

[29] R. B. White, *Theory of Toroidally Confined Plasmas*, 3rd ed. (Imperial College Press, London, 2014).

[30] See Supplemental Material at http://link.aps.org/supplemental/10.1103/j3cm-5mtm for an animated version of Figure 5.

[31] J. W. Connor, R. O. Dendy, R. J. Hastie, D. Borba, G. Huysmans, W. Kener, and S. Sharapov, Non-ideal effects on toroidal Alfvén eigenmode stability, in *Proceedings of 21st EPS Conference* (EPS, Geneva, 1994), Vol. 18B, p. 616.

[32] P. Rodrigues, A. Figueiredo, J. Ferreira, R. Coelho, F. Nabais, D. Borba, N. F. Loureiro, H. J. C. Oliver, and S. E. Sharapov, Systematic linear-stability assessment of Alfvén eigenmodes in the presence of fusion α-particles for ITER-like equilibria, Nucl. Fusion **55**, 083003 (2015).

[33] A. C. A. Figueiredo, P. Rodrigues, D. Borba, R. Coelho, L. Fazendeiro, J. Ferreira, N. F. Loureiro, F. Nabais, S. D. Pinches, A. R. Polevoi, and S. E. Sharapov, Comprehensive

evaluation of the linear stability of Alfvén eigenmodes driven by alpha particles in an ITER baseline scenario, Nucl. Fusion **56**, 076007 (2016).
[34] R. R. Mett and S. M. Mahajan, Kinetic theory of toroidicity-induced Alfvén eigenmodes, Phys. Fluids B **4**, 2885 (1992).
[35] N. N. Gorelenkov and S. E. Sharapov, On the collisional damping of TAE-modes on trapped electrons in tokamaks, Phys. Scr. **45**, 163 (1992).
[36] A. Hasegawa and L. Chen, Kinetic processes in plasma heating by resonant mode conversion of Alfvén wave, Phys. Fluids (1958–1988) **19**, 1924 (1976).
[37] Y. Omura, H. Matsumoto, T. Miyake, and H. Kojima, Electron beam instabilities as generation mechanism of electrostatic solitary waves in the magnetotail, J. Geophys. Res. **101**, 2685 (1996).
[38] P. C. Filbert and P. J. Kellogg, Electrostatic noise at the plasma frequency beyond the Earth's bow shock, J. Geophys. Res. **84**, 1369 (1979).
[39] D. V. Dylov and J. W. Fleischer, Observation of all-optical bump-on-tail instability, Phys. Rev. Lett. **100**, 103903 (2008).
[40] M. C. Herrmann and N. J. Fisch, Cooling energetic α particles in a tokamak with waves, Phys. Rev. Lett. **79**, 1495 (1997).
[41] J. Riemann, S. Vaz Mendes, K. Rahbarnia, R. Kleiber, C. Slaby, A. Könies, M. Borchardt, A. Mishchenko, H. Thomsen, C. Büschel, A. von Stechow, J.-P. Bähner, S. K. Hansen, E. Edlund, and Wendelstein 7-X Team, Excitation of Alfvénic modes via electromagnetic turbulence in Wendelstein 7-X, Phys. Rev. Lett. **134**, 025103 (2025).